Liquid Crystals
Publication details, including instructions for authors and subscription information:
http://www.informaworld.com/smpp/title~content=t713926090

Thermal study of the influence of aerosils on the phase transitions of heptyloxybenzylidene butylaniline

H. Haga; C. W. Garland

Online publication date: 29 June 2010

To cite this Article Haga, H. and Garland, C. W.(1997) 'Thermal study of the influence of aerosils on the phase transitions of heptyloxybenzylidene butylaniline', Liquid Crystals, 23: 5, 645 — 652
To link to this Article: DOI: 10.1080/026782997207911
URL: http://dx.doi.org/10.1080/026782997207911

LIQUID CRYSTALS, 1997, VOL. 23, NO. 5, 645–652

Thermal study of the influence of aerosils on the phase transitions of heptyloxybenzylidene butylaniline

by H. HAGA and C. W. GARLAND*

School of Science and Center for Material Science and Engineering, Massachusetts Institute of Technology, Cambridge, Massachusetts 02139, U.S.A.

(*Received 29 April 1997; accepted 28 May 1997*)

Bulk heptyloxybenzylidene butylaniline (7O.4) undergoes first order nematic (N)–isotropic (I), nematic–smectic A (SmA), and smectic C (SmC)–crystal G(CrG) transitions as well as a mean-field second order SmA–SmC transition. The dispersion of 70 Å diameter hydrophobic silica aerosil particles in 7O.4 leads to doubling and significant temperature shifts for all three first order transitions, as determined with a.c. calorimetry. The SmA–SmC heat capacity peak merely shifts in position while remaining a single sharp Landau feature with an amplitude that decreases as the aerosil density increases. The behaviour of three 7O.4 + hydrophobic aerosil samples is discussed and compared to that of one 7O.4 + hydrophilic aerosil and previously reported results for 7O.4 + aerogel and 4O.8 + aerosil samples.

1. Introduction

Much work has been done in the past five years on the effects of porous networks on the phase behaviour of thermotropic liquid crystals [1]. Included in that effort are studies of liquid crystals (LC) in silica aerogels [1–4]. Recently two calorimetric studies have been carried out on the effects of small (70 Å) dispersed silica aerosil particles on the phase transitions in octylcyanobiphenyl (8CB) [5] and butyloxybenzlidene octylaniline (4O.8) [6]. The principal focus of that aerosil work was changes in the critical exponent α associated with the second order nematic (N)–smectic A (SmA) transition.

The present investigation involves a high-resolution calorimetric study of aerosil effects on *N*-(4-*n*-heptyloxybenzilidene)-4′-*n*-butylaniline (7O.4) with molecular weight 351·5 g mol^{-1} and structural formula

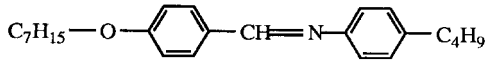

This compound exhibits the phase sequence

$$\mathrm{CrK}\ \underset{305{\cdot}2\,\mathrm{K}}{\overline{\qquad}}\ \mathrm{CrG}\ \underset{336{\cdot}2\,\mathrm{K}}{\overline{\qquad}}\ \mathrm{SmC}\ \underset{337{\cdot}6\,\mathrm{K}}{\overline{\qquad}}$$

$$\mathrm{SmA}\ \underset{347{\cdot}20\,\mathrm{K}}{\overline{\qquad}}\ \mathrm{N}\ \underset{349{\cdot}35\,\mathrm{K}}{\overline{\qquad}}\ \mathrm{I}$$

where I, SmC, CrG and CrK denote isotropic, smectic C, plastic crystal G and rigid crystal K, respectively, and the transition temperatures are taken from Refs [7, 8]. All of the transitions except for SmA–SmC are first order. The SmC–CrG and CrG–CrK transitions in bulk 7O.4 are strongly first order, and the SmC–CrG transition exhibits only small pretransition C_p wings. The N–I and N–SmA bulk transitions are clearly first order but exhibit significant pretransitional C_p wings. The reason that the N–SmA transition is first order in 7O.4, whereas it is second order in many LCs including most *n*O.*m* compounds (even 4O.7), is the narrow nematic range. A well-understood deGennes coupling between the smectic order parameter ψ and nematic order parameter S can drive the N–SmA transition first order via a tricritical point when the nematic range is narrow (and hence the nematic susceptibility is large) [9]. The SmA–SmC transition is mean-field second order and well described by the so-called extended Landau model [8]. Indeed, the bulk SmA–SmC transition is close to a classical Landau tricritical point and exhibits a large C_p peak. Thus this is the first study of the effect of aerosil particles on a first order N–SmA transition or a mean-field SmA–SmC transition.

Section 2 describes the experimental procedures and reports the results of C_p measurements on bulk 7O.4 and four 7O.4 + aerosil samples. Included in this section in a mean-field analysis of the excess heat capacity associated with the SmA–SmC transition and its evolution as a function of aerosil perturbation. In § 3, comparisons will be made with recent results for 7O.4 in silica aerogels [10] and for 8CB + aerosil and 4O.8 + aerosil systems [5, 6].

2. Experimental procedures and results

The 7O.4 used in the present work was obtained from M. E. Neubert of Kent State University and was used without further purification. Two types of aerosil from

*Author for correspondence.

Degussa Corporation were used. Both are 70 Å diameter SiO_2 spheres, but the hydrophilic (type 300) has surface OH groups and the hydrophobic (type R812) has surface CH_3 groups [11].

The LC + aerosil samples were prepared by a new method which involves adding the sil to a dilute solution of 7O.4 in ethanol, sonicating to achieve good dispersion, and then slowly evaporating off the solvent. Further details are given in Ref. [6]. Recent SAXS (small angle X-ray scattering) data show that aerosils dispersed in a LC exhibit fractal structures very similar to those seen in aerogels [12]. For 8CB + aerosils prepared by mechanical mixing, dispersions of philic sils and phobic sils seem to behave in a very similar manner [5]. For 4O.8 + aerosils prepared in the same manner as the present systems, five philic sil dispersions and one phobic sil dispersion were studied [6]. It was discovered that phobic sil particles disperse better (more uniformly, without visible gradients) in 7O.4 than do philic sil particles, which become inhomogeneous at moderate densities. Thus only one philic sil system with $\rho_s = 0{\cdot}019\,\mathrm{g\,cm^{-3}}$ was studied, whereas three phobic sil dispersions with ρ_s values from 0·024 to $0{\cdot}139\,\mathrm{g\,cm^{-3}}$ were investigated. The density ρ_s quoted in this paper denotes grams of SiO_2 per cm^3 of LC.

After a sample was prepared, it was cold-weld sealed into a silver cell (~1 cm diameter and ~1 mm thick), and the filled cell was mounted in a high-resolution a.c. calorimeter described elsewhere [13]. See Ref. [6] for further experimental details and Ref. [14] for the equations for processing the observed responses—$T_{a.c.}$ and $\phi \equiv \Theta + \pi/2$, where Θ is the phase shift of $T_{a.c.}$ with respect to the input power $P_{a.c.}\exp(i\omega t)$. The essential equations, valid in the absence of two-phase coexistence, are

$$C_p = [C'_{filled} - C_{empty}]/m \qquad (1)$$

$$= \left[\frac{|P_{a.c.}|}{\omega|T_{a.c.}|}\cos\phi - C_{empty}\right] \Big/ m,$$

$$C''_{filled} = \frac{|P_{a.c.}|}{\omega|T_{a.c.}|}\sin\phi - \frac{1}{\omega R} = 0, \qquad (2)$$

where C'_{filled} and C''_{filled} are the real and imaginary components of the heat capacity, C_{empty} is the heat capacity of the empty silver cell, m is the mass of LC in grams, and R is the thermal resistance between sample cell and the bath. All measurements were made at $\omega_o/2$, where $\omega_o = 0{\cdot}196\,\mathrm{s^{-1}}$ is the standard frequency used for most previous work with this calorimeter. Measurements at such a low frequency ($f = 15{\cdot}63$ mHz) should yield the static thermodynamic heat capacity. Note that dips in $\tan\phi$ are expected when C'_{filled} exhibits a peak and there is no two-phase coexistence or intrinsic dynamics (so that $C''_{filled} = 0$). Under those conditions,

$$\tan\phi = 1/\omega R C'_{filled}. \qquad (3)$$

The heat capacity and a.c. phase shifts for 7O.4 are shown in figure 1. The abrupt pronounced spikes in $\tan\phi$ are characteristic of regions of two-phase coexistence [3, 13, 15], and the artificial C_p values obtained in such regions are denoted by crosses. The data in figure 1 were obtained on a cooling run in which the sample temperature was scanned at $-50\,\mathrm{mK\,h^{-1}}$ near the SmA–SmC transition and faster (but less than $250\,\mathrm{mK\,h^{-1}}$) elsewhere. The N–I coexistence region was 213 mK wide and centred at 349·361 K; the N–SmA coexistence region was 293 mK wide and centred at 347·162 K; and the SmA–SmC second order transition temperature was 337·665 K. The SmC–CrG freezing transition was ~1·4 K wide and can be characterized by two temperatures: the C_p maximum observed on cooling was at 336·265 K, and the position of the abrupt jump in the apparent C_p (marking the first appearance of two phases on cooling) was at 336·372 K. These transition temperatures are in excellent agreement with those given in Refs [7] and [8]. The bulk 7O.4 (and 7O.4 + aerogel)

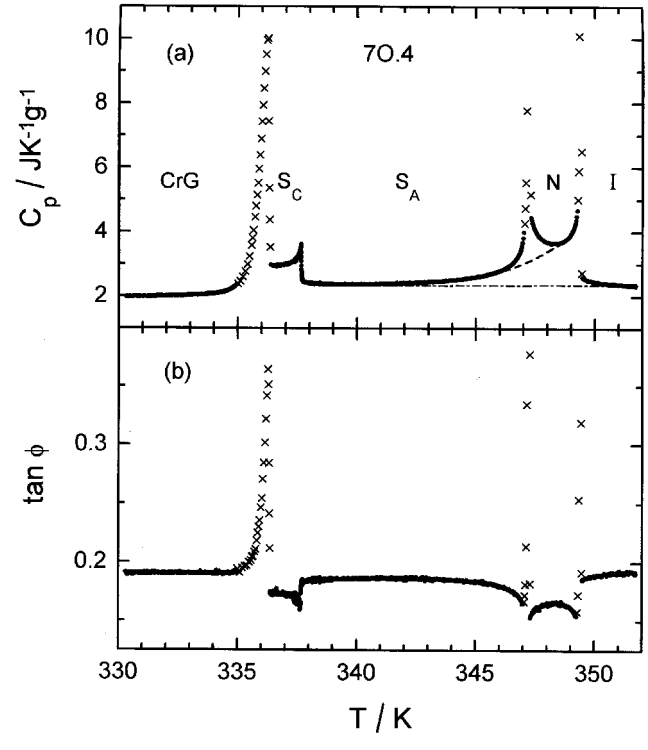

Figure 1. (*a*) Heat capacity for bulk 7O.4. The C_p points indicated by a cross (×) are artificial values obtained in a two-phase coexistence region. The dashed lines indicate the pretransitional N–I wings. (*b*) $\tan\phi$ variation for 7O.4. Dips are expected in one-phase regions when there are C_p peaks, see equation (3). The large spikes in $\tan\phi$ are the characteristic anomalies observed at first order transitions.

transition temperatures reported in [10] are systematically low by ~1·1 K due to a thermistor calibration error. Luckily, that does not affect the values of the shifts T_t(gel)–T_t(bulk) in transition temperatures between bulk 7O.4 and 7O.4 + aerogel samples that can be obtained from [10].

The heat capacity C_p and the phase shift $\tan\phi$ are given in figure 2 for the 7O.4 + phobic sil sample with $\rho_s = 0{\cdot}080\,\mathrm{g\,cm^{-3}}$. The features shown here are typical of the phobic sil samples: all first order bulk transitions are doubled and remain first order, while the second order SmA–SmC transition remains a single sharp feature; and all transition temperatures are appreciably shifted relative to their bulk values.

Figure 3 gives a detailed view of $C_p(T)$ in the I–N–SmA region for all the samples investigated, and a comparable detailed view of the SmA–SmC–CrG region is given in figure 4. Included in these figures are pure bulk 7O.4, one philic sil sample, and three phobic sil samples. Note that the qualitative behaviour at the N–SmA and SmC–CrG transitions is different for the philic sil sample in that these C_p peaks are asymmetrically broadened on the low temperature side but there is

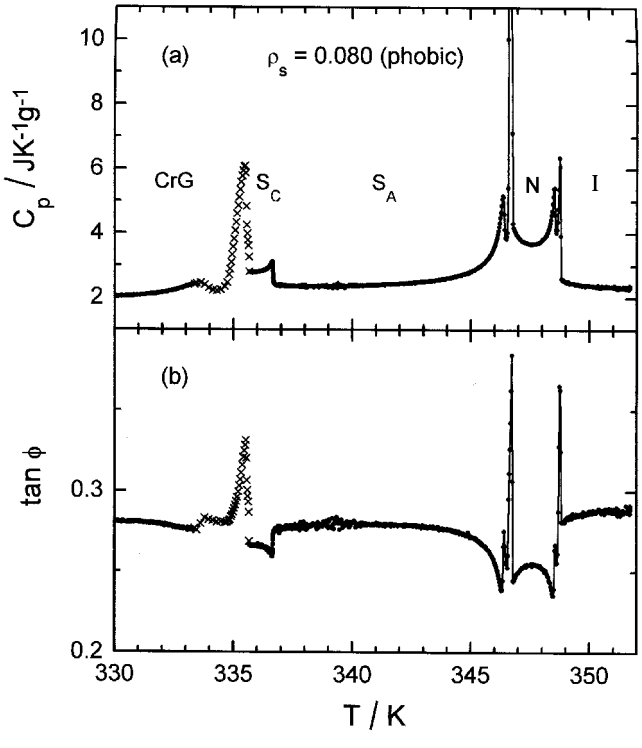

Figure 2. (*a*) Heat capacity of 7O.4 + aerosil for a phobic sil sample with density $\rho_s = 0{\cdot}080\,\mathrm{g\,cm^{-3}}$. (*b*) $\tan\phi$ variation for this sample. Note that both C_p and $\tan\phi$ peaks are doubled for first order transitions. The symbol × denotes a point in a two-phase SmC–CrG coexistence region. For clarity, × symbols are not used for the doubled N–I or N–SmA transitions although these are also first order.

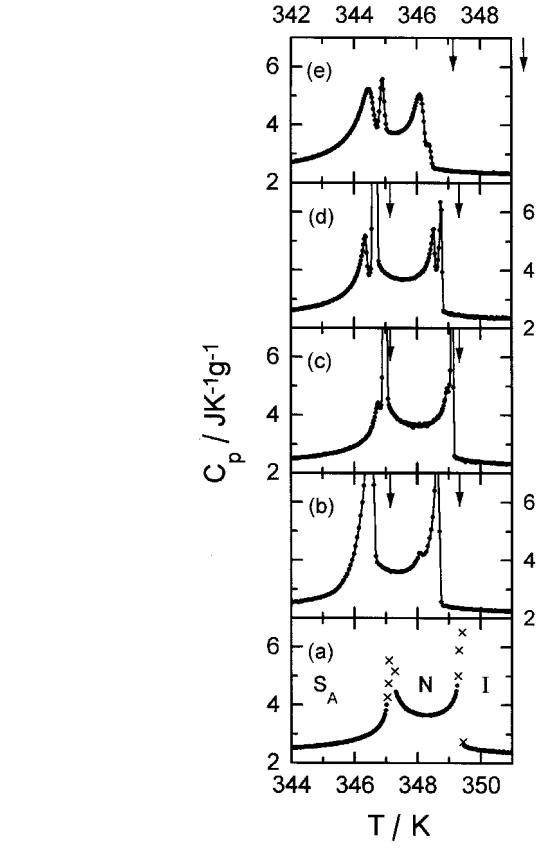

Figure 3. Detailed view of C_p in the I–N–SmA region for bulk 7O.4 and 7O.4 + aerosil samples with silica densities $\rho_s = 0$ (*a*), 0·019 philic (*b*), 0·024 phobic (*c*), 0·080 phobic (*d*), and 0·139 phobic (*e*). Because of the large shift in transition temperatures for $\rho_s = 0{\cdot}139$, the T scale is shifted in this case. For every sil sample, the arrows at the top of the box indicate the position of the transition in bulk 7O.4. All the sil peaks are first order with pretransitional wings (see figure 2).

no obvious doubling. Also the $\tan\phi$ dips below the N–I transition and both above and below the N–SmA transition seen for phobic sil samples (for example, figure 2) are missing for this philic sil sample.

Table 1 summarizes the coexistence widths and the transition temperature shifts relative to bulk 7O.4, and figure 5 displays the trends in the N–I, N–SmA, and SmA–SmC transition temperatures. Since the latent heats associated with the first order transitions are not known and it is difficult to separate pretransitional C_p wings for the N–I and N–SmA transitions, transition enthalpies for LC + sil samples are not given in table 1.

It is clear from figure 4 that the second order SmA–SmC transition is mean-field-like in all the phobic sil samples. Thus we have carried out fitting with the Landau model based on a free energy with the usual mean-field form

$$G = G_o + at\theta^2 + b\theta^4 + c\theta^6, \qquad (4)$$

where G_o is the "disordered" (background) Gibbs free energy, θ is the magnitude of the tilt order parameter, $t \equiv (T - T_c)/T_c$ is the reduced temperature, and all the coefficients a, b, c are positive for a second order transition. Equation (4) yields for the heat capacity [8]

$$\Delta C_p = C_p - C_{po} = \begin{cases} 0 & \text{for } T > T_c, \quad (5a) \\ A \dfrac{T}{T_c} \left(\dfrac{T_m - T_c}{T_m - T} \right)^{1/2} & \text{for } T < T_c, \quad (5b) \end{cases}$$

where $A \equiv a^2/2bT_c$, $T_m \equiv T_c + (b^2 T_c/3ac)$ is the metastability limit, and C_{po} is the background heat capacity. Another convenient form of equation (5b), if one takes T/T_c as a constant equal to unity over a narrow SmC range, is

$$\Delta C_p = A^* (T_m - T)^{-1/2} \quad \text{for } T < T_c, \qquad (6)$$

where $A^* = (a^3/2c\,T_c)^{1/2}$ [16]. This form stresses the fact that T_c does not influence the *shape* of the ΔC_p curve; its only role is to determine the position of the jump in ΔC_p.

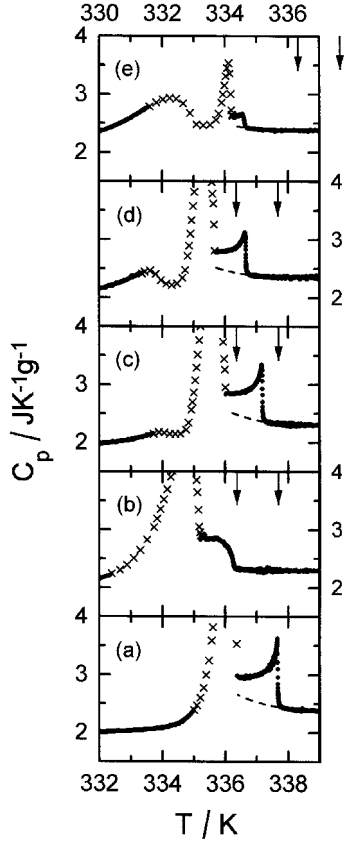

Figure 4. Detailed view of C_p in the SmA–SmC–CrG region for bulk 7O.4 and 7O.4 + aerosil samples with silica densities ρ_s the same as those defined in figure 3. Since the bulk SmC–CrG coexistence region is wide, the arrow in this case indicates the position of the jump in C_p(bulk) on the high temperature side of this coexistence region. The dashed lines are C_p(background) curves chosen for the analysis of the SmA–SmC transition region.

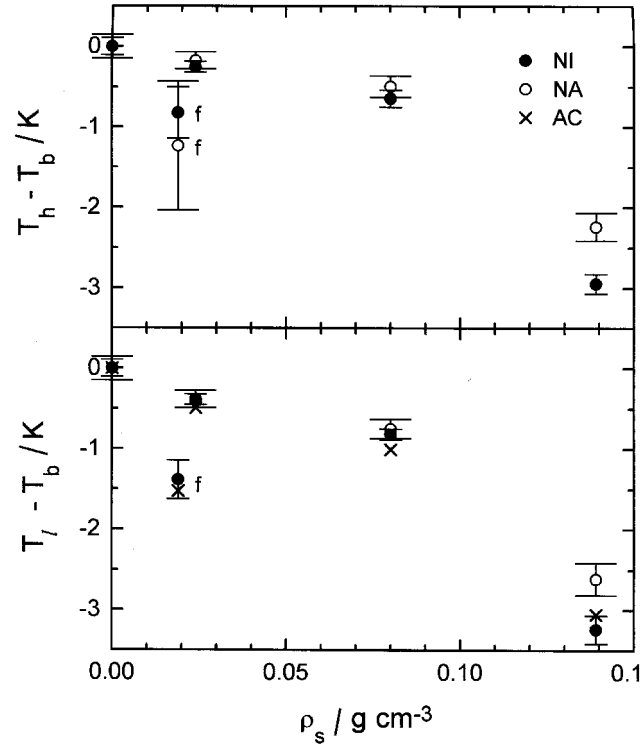

Figure 5. Shifts in transition temperatures from those for bulk 7O·4. (*a*) $\Delta T = T_{high} - T_{bulk}$ for the high-T component of the doubled N–I (●) and N–SmA (○) transitions in 7O.4 + phobic aerosils of density ρ_s. (*b*) $\Delta T = T_{low} - T_{bulk}$ for the low-T component of N–I (●) and N–SmA (○) transitions and for the SmA–SmC transition (+). Points marked with f are for the one philic aerosil sample. The vertical bars denote the coexistence widths for the N–I and N–SmA transitions.

The background contribution is usually a linear and slowly varying function of temperature, $B + E(T - T_c)$ with E equal to zero or a small positive number. However, the SmA–SmC transition in *n*O.*m* compounds is close to the freezing transition into a 3D plastic crystal phase, and it is known that there is a small pretransitional increase in C_p associated with smectic–plastic crystal transitions [17]. Thus the C_{po} line in the present situation is curved and has a negative slope; see Ref. [8] for more details. C_{po} curves are shown in figure 4 for all the phobic sil samples. In the case of the one philic sil, the SmA–SmC excess heat capacity is too rounded to allow any fitting.

The fitting parameters obtained from least-squares fits of our SmA–SmC excess heat capacity data with equation (5) are given in table 2, and one fit is shown in figure 6 as a typical example. Also given in table 2 are the parameters for bulk 7O.4 given in Ref. [8], which

Table 1. Shifts in transition temperatures for 7O.4 + aerosils relative to bulk 7O.4 and two-phase coexistence widths, both in K. In the case of the SmC–CrG transition, where the coexistence region is very broad, ΔT values for the high temperature components were determined using the position of the abrupt rise in C_p on cooling. For bulk 7O.4, $T_{NI} = 349{\cdot}361$ K and $T_{NA} = 347{\cdot}162$ K (both centres of coexistence regions), $T_{AC} = 337{\cdot}665$ K, and $T_{CG} = 336{\cdot}372$ K (jump in C_p on cooling) or 336·265 K (position of C_p maximum on cooling). Since all the first order transitions for phobic sil systems were doubled, there are two entries $\Delta T(h)$ and $\Delta T(l)$ for the high and low temperature components. The density ρ_s is g of SiO_2 per cm^3 of LC.

Sample	ρ_s	NI coex.	$\Delta T_{NI}(h)$	$\Delta T_{NI}(l)$	NA coex.	$\Delta T_{NA}(h)$	$\Delta T_{NA}(l)$	ΔT_{AC}	CG coex.	$\Delta T_{CG}(h)$	$\Delta T_{CG}(l)$
bulk	0	0·213	0	0	0·293	0	0	0	~1·40	0	0
sil(philic)	0·019	1·12	−0·82	−1·38	1·60	−1·23		−1·536	~3·0	−1·05	
sil(phobic)	0·024	0·266	−0·25	−0·39	0·422	−0·18	−0·38	−0·489	~2·3	−0·35	−2·36
	0·080	0·346	−0·64	−0·82	0·508	−0·49	−0·75	−1·004	~2·3	−0·69	−2·65
	0·139	0·586	−2·94	−3·24	0·747	−2·24	−2·61	−3·052	~2·7	−2·12	−4·03

Table 2. Parameter values obtained from least-squares fitting ΔC_p(SmA–SmC) data with equation (5) for 7O.4 and 7O.4 + phobic aerosils with silica densities ρ_s in $g\,cm^{-3}$. Quantities in brackets were held fixed at the given value. The units of A are $J\,K^{-1}\,g^{-1}$. The values of t_{min} are $t_{min}^{+} \simeq 4 \times 10^{-4}$ and $t_{min}^{-} \simeq -10^{-4}$; the values of t_{max} are $t_{max}^{+} = 1{\cdot}5 \times 10^{-3}$ and $t_{max}^{-} = -3 \times 10^{-3}$ except for $\rho_s = 0{\cdot}139$ where $t_{max}^{-} = 10^{-3}$ due to the diminished width of the SmC range. The quantity t_o is given for convenience but is not a fitting parameter. The first two lines are fits taken from [8] for the sample studied there.

Fit	Sample	ρ_s	A	T_m/K	T_c/K	$10^3 t_o$	C_{po}^{a}	χ_ν^2
[8]	Bulk	0	1·126	337·655	[337·559]	0·9	c	1·54
[8]		0	1·131	337·646	[337·559]	0·8	/	1·28
1	Bulk	0	1·157	337·790	[337·665]	1·1	c	1·39
2		0	1·163	337·778	[337·665]	1·0	/	1·03
3	Sil 1	0·024	1·057	337·292	[337·176]	1·0	c	1·45
4		0·024	1·059	337·280	[337·176]	0·9	/	1·00
5	Sil 2	0·080	0·812	336·789	[336·661]	1·1	c	1·05
6		0·080	0·819	336·774	[336·661]	1·0	/	1·03
7	Sil 3	0·139	0·263	334·803	[334·613]	1·7	c	0·98
8		0·139	0·259	334·827	[334·613]	1·9	/	1·00

[a] The letter c denotes a curved background like the dot–dash curve in figure 6, and / denotes a linear background like the dashed line in figure 6.

are in good agreement with the present bulk fits. The quantity $t_o \equiv 3(T_m - T_c)/T_c = b^2/ac$ is a convenient measure of the closeness to classical tricriticality. The excess heat capacity ΔC_p jumps discontinuously from 0 to A at T_c; this excess has a value $A/2$ at $t = -t_o$. Thus t_o characterizes the sharpness of the ΔC_p peak and $t_o = 0$ (or $b = 0$) correspond to a mean-field tricritical point [16].

3. Discussion

The first thermal study of the effects of aerosils on LC phase transitions was carried out on 8CB, in which case philic and phobic sils produced the same effects [5]. A recent study of 4O.8 + aerosil samples involved mostly philic sils [6]. Although the effects on the shapes of the second order ΔC_p(N–SmA) peaks were comparable to those observed for 8CB, the shifts in transition temperatures were much larger for 4O.8. Moreover, the present data make it clear that 7O.4 is differently affected by phobic and philic sil particles. Such differences between 8CB and presumably all nO.m compounds are not surprising since nO.m can hydrogen bond to the hydroxyl groups on the philic sil surface whereas 8CB cannot. In the case of phobic sils with surface CH_3 groups, no specific interaction like hydrogen bonding can occur for any LC. Thus the 8CB–sil interaction is not sensitive to the sil surface character, but the 7O.4–sil (and 4O.8–sil) interaction differs greatly for philic and phobic surfaces. The greater anchoring of 7O.4 to a philic sil surface would explain the larger shifts in transition temperatures for a given ρ_s and the greater broadening and rounding of all the philic C_p peaks. The fact that the transition temperature shifts are negative for both types of sil indicates that philic and phobic silica acts as a disordering surface [18].

A very interesting feature of the present data is the doubling of all three first order transitions but not of the second order SmA–SmC transition. This seems to be a fairly general phenomena which will be discussed below in the context of comparing 7O.4 + aerosil behaviour for individual transitions with the behaviour of other LC + sil samples. Both components of a doubled first

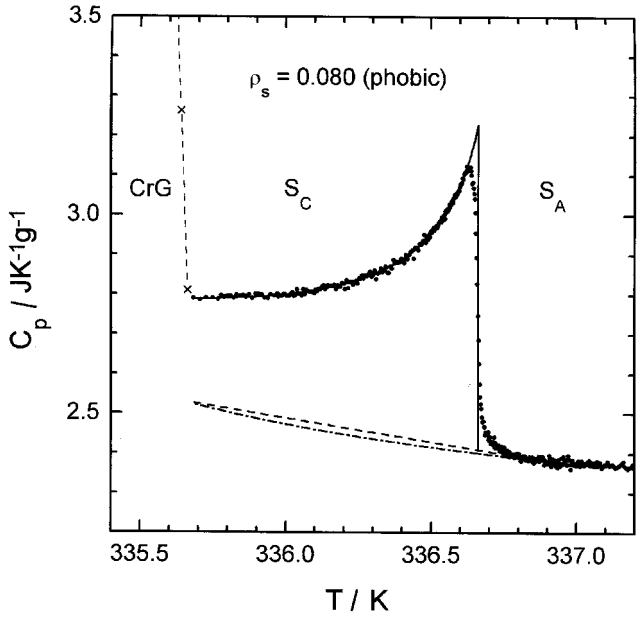

Figure 6. Heat capacity near the SmA–SmC transition in the 7O.4 + aerosil sample with $\rho_s = 0{\cdot}080\,\mathrm{g\,cm^{-3}}$. The dot–dash curve for C_p(background) is based on the type of analysis discussed in the text and in [8]. The linear dashed C_p(background) has also been used for fits to ΔC_p. The solid line is Landau fit 6 from table 2.

order transition have fairly sharp C_p features (especially the high-T component) that are appreciably shifted from the bulk 7O.4 temperatures. Given the fact that this doubling occurs at very low silica densities, some long range force must be involved, like orientational elastic effects. If elastic effects (say bend and splay in the nematic region for example) play a major role in introducing defects and dislocations into the liquid crystal due to effects of the surface, any ordering must be influenced by such elastic defects. However, as the sample is cooled and becomes stiffer it will become energetically favourable to reduce or modify such defects (with perhaps rotational motion of some sil particles), which will allow a substantial increase in ordering to occur at a second and lower temperature. However, unlike first order transitions where two distinct free energy surfaces intersect there is only a single free energy surface in the case of second order transitions, and perturbations can shift and even smear the associated C_p peak (proportional to $\partial^2 G/\partial T^2$) but not double it. A detailed discussion of elastic perturbation effects will be given elsewhere [19].

One feature of nO.m + aerosil samples that is not presently understood is the fact that 4O.8 + philic sil samples can be prepared with good homogeneity up to a silica density ρ_s of $0{\cdot}438\,\mathrm{g\,cm^{-3}}$, whereas 7O.4 + philic sil samples exhibit visible heterogeneities and even some agglomeration for $\rho_s \geqslant 0{\cdot}02\,\mathrm{g\,cm^{-3}}$.

3.1. *N–I transition*

The N–I transition in bulk 7O.4 has a large latent heat ΔH ($\sim 4{\cdot}4\,\mathrm{J\,g^{-1}}$ from DSC data [7]) relative to bulk 4O.8 ($\Delta H \simeq 3{\cdot}36\,\mathrm{J\,g^{-1}}$ [4]) and bulk 8CB ($\Delta H \simeq 2{\cdot}10\,\mathrm{J\,g^{-1}}$ [3]). In the latter cases, there are appreciable pretransitional N–I heat capacity wings and their integrated areas δH_{NI} are $4{\cdot}30\,\mathrm{J\,g^{-1}}$ for 4O.8 [3] and $5{\cdot}58\,\mathrm{J\,g^{-1}}$ for 8CB [3]. The quantity δH is defined by

$$\delta H = \int \Delta C_p \, \mathrm{d}T, \tag{7}$$

where the excess heat capacity ΔC_p is $C_p - C_p$ (background); see Ref. [6] for further details. Our best estimate of δH_{NI} for 7O.4 is based on the dashed lines in figure 1 and has the value $5{\cdot}71\,\mathrm{J\,g^{-1}}$. Thus the total N–I enthalpy $\Delta H + \delta H$ is larger ($\sim 10\,\mathrm{J\,g^{-1}}$) for 7O.4 than for the other two liquid crystals ($\sim 7{\cdot}7\,\mathrm{J\,g^{-1}}$).

The conspicuous doubling of the N–I C_p peak shown in figures 2 and 3 for 7O.4 + aerosil samples is also observed for 8CB + aerosils [5, 19] but is not seen for 4O.8 + philic aerosils, where only a tiny secondary high temperature peak is observed for the $\rho_s = 0{\cdot}23$ sample [6]. In silica aerogels, no N–I doubling of C_p(ac) occurs for 8CB, 4O.8 or 7O.4 if one neglects a very small and narrow peak due to a slight surface excess of bulk LC [2, 4, 10]. Further discussion of this N–I doubling in LC + aerosil samples will be given in Ref. [19].

3.2. *N–SmA transition*

In 8CB + aerosil and 4O.8 + aerosil samples, the N–SmA transition is second order and exhibits singular C_p peaks without significant rounding for $\rho_s \lesssim 0{\cdot}09\,\mathrm{g\,cm^{-3}}$ [5, 6]. As ρ_s increases, the ΔC_p(N–SmA) peak undergoes crossover from the bulk power-law shape with an effective critical exponent $\alpha_{bulk} > 0$ to a 3D–XY shape with $\alpha \simeq \alpha_{XY} = -0{\cdot}007$, presumably due to a change in smectic–nematic order parameter coupling related to a decrease in the nematic susceptibility. The N–SmA transition in 7O.4 is strongly first order and remains first order for 7O.4 + aerosil samples (at least up to $\rho_s = 0{\cdot}139\,\mathrm{g\,cm^{-3}}$). Thus theoretical predictions that first order transitions become continuous as a result of a quenched random field [20] are not fulfilled for either the N–I or N–SmA transitions in 7O.4 + aerosil samples. Either the theoretical model is flawed or inapplicable to such aerosil systems (which are probably not completely quenched [19]), or perhaps the perturbation due to aerosil randomness is too weak when $\rho_s \lesssim 0{\cdot}14\,\mathrm{g\,cm^{-3}}$ to eliminate the first order character.

For all the investigated 7O.4 + phobic aerosil samples, the N–SmA transition is doubled in a manner almost exactly the same as for the N–I transition. In contrast,

the one 7O.4 + philic aerosil exhibits a single C_p peak at the N–SmA transition. However, this C_p(N–SmA) peak is asymmetrically broadened on the low-temperature side, as in the $\tan\phi$ anomaly which exhibits a shoulder below the main peak (not shown). This suggests that two N–SmA peaks may exist but they overlap so extensively that a double feature is not resolvable with a.c. calorimetry. In aerogels containing 7O.4, the N–SmA transition is first order and there is a single very broad C_p(N–SmA) peak [10].

3.3. *SmA–SmC transition*

This second order transition yields a single Landau C_p peak in 7O.4 + phobic sil samples. The lack of doubling here is consistent with the absence of doubling for second order peaks in 8CB and 4O.8 aerosil samples (in those cases, fluctuation type N–SmA transitions). The size and sharpness (the quantities A and t_o in table 2) of the SmA–SmC peaks evolve smoothly with silica density ρ_s. The deviations from a Landau fit, visible in figure 6, are of two kinds. The small pretransitional C_p wing for $T > T_c$ was constant in size and shape for all 7O.4 + phobic aerosil samples, and the same feature was seen for bulk 7O.4 (and, indeed, for several bulk nO.m materials [8]). The rounding of C_p values at the peak of ΔC_p (SmA–SmC) is an aerosil effect. This rounding does not occur for our bulk 7O.4 sample nor for that studied in Ref. [8]. Furthermore, this peak rounding is proportional to the aerosil density—visible but much smaller for $\rho_s = 0{\cdot}024$ but clearly larger for $\rho_s = 0{\cdot}139$. This fits in with our suggestion that perturbations can shift and round off a second order C_p peak but not double it.

Note that figure 4 shows that the C_p (SmA–SmC) feature is heavily rounded and step-like in the one 7O.4 + philic sil sample at the low density $\rho_s = 0{\cdot}019\,\mathrm{g\,cm^{-3}}$. The phase quantity $\tan\phi$ still exhibits a second order type dip but also rounded (not shown). One possibility is that the philic aerosil has greatly altered the Landau free energy coefficients b and c in equation (4) by increasing b and decreasing c (due to hydrogen bonding perhaps). This would make t_o much larger than the values given in table 2, which means that C_p (SmA–SmC) could change from a sharp peak to a classic mean-field step-like feature similar to that observed at SmA_2–SmC_2 transitions in bulk liquid crystals [21]. No SmA–SmC transition can be observed for 7O.4 confined in aerogels of density $\rho(\mathrm{gel}) = 0{\cdot}08$ and $0{\cdot}17\,\mathrm{g\,cm^{-3}}$ [10]. The density ρ_s for a gel is $\rho(\mathrm{gel})/\phi_p$, where ϕ_p is the volume fraction of pores [3]; thus $\rho_s = 0{\cdot}085$ and 0·19 for these two aerogels. We believe that this is consistent with the present data in that the rounded and somewhat smeared SmA–SmC peak seen for 7O.4 + philic aerosil with $\rho_s = 0{\cdot}019$ could be completely suppressed if one would increase ρ_s to $\sim 0{\cdot}08$ with a philic sil. More work on 7O.4 in aerogels of lower density (if they will support being filled with a LC) or higher density 7O.4 + philic aerosil samples (if a method of preparation can be found) would be of value in bridging the present density gap.

3.4. *SmC–CrG transition*

Like the other 7O.4 first order transitions, the SmC–CrG transition in 7O.4 + phobic sil samples is doubled and both components remain first order. In this case, however, the temperature difference between components is much larger ($\sim 1{\cdot}9$ K between centres of the two components compared to 0·13–0·29 K for N–I and 0·21–0·37 K for N–SmA). As with the N–SmA transition, the 7O.4 + philic sil sample exhibits a single C_p (SmC–CrG) peak broadened appreciably on the lower temperature side and the same is true for 7O.4 confined in aerogels, which also have philic hydroxyl surfaces [10]. This freezing behaviour of LCs in contact with SiO_2 aerosil surfaces is confirmed by the SmA–CrB data on 4O.8 + aerosils [6]: the SmA–CrB C_p peak is a single feature for philic sils but is doubled for 4O.8 + phobic sils. No comparison is possible with 8CB + sils or gels since freezing, which occurs at ~ 270 K, has not been studied calorimetrically.

The authors wish to thank G. S. Iannacchione and F. D. Greene for helpful discussions. This work was supported by NSF grant DMR 93-11853.

References

[1] 1996, *Liquid Crystals in Complex Geometries Formed by Polymer and Porous Networks*, edited by G. P. Crawford and S. Zumer (London: Taylor & Francis), and references therein.

[2] Bellini, T., Clark, N. A., and Schaefer, D. W., 1995, *Phys. Rev. Lett.*, **74,** 2740.

[3] Wu, L., Zhou, B., Garland, C. W., Bellini, T., and Schaefer, D. W., 1995, *Phys. Rev. E*, **51,** 2157, and references cited therein.

[4] Kutnjak, Z., and Garland, C. W., 1997, *Phys. Rev. E*, **55,** 488.

[5] Zhou, B., Iannacchione, G. S., Garland, C. W., and Bellini, T., 1997, *Phys. Rev. E*, **55,** 2962.

[6] Haga, H., and Garland, C. W., 1997, *Phys. Rev.*, **E56,** Sept.

[7] (*a*) Smith, G. W., Gardlund, Z. G., and Curtis, R. J., 1973, *Mol. Cryst. liq. Cryst.*, **19,** 327; (*b*) Smith, G. W., and Gardlund, Z. G., 1973, *J. chem. Phys.*, **59,** 3214.

[8] Meichle, M., and Garland, C. W., 1983, *Phys. Rev. A*, **27,** 2624.

[9] Thoen, J., 1992, in *Phase Transitions in Liquid Crystals*, Vol. 290 of NATO *Advanced Study Institute, Series B; Physics*, edited by S. Martellucci and A. N. Chester (Plenum, New York), pp. 155–174.

[10] Haga, H., and Garland, C. W., 1997, *Liq. Cryst.* **22,** 275.
[11] Degussa Corp., Silica Division, 65 Challenger Rd, Ridgefield Park, NJ 07660, U.S.A.
[12] Iannacchione, G. S., private communication.
[13] (*a*) Garland, C. W., 1985, *Thermochim. Acta*, **88,** 127; (*b*) *Liquid Crystals: Physical Properties and Phase Transitions*, edited by S. Kumar (Oxford University Press, New York), Chap. 6, in press.
[14] Yao, H., Chan, T., and Garland, C. W., 1995, *Phys. Rev. E*, **51,** 4585.
[15] Wen, X., Garland, C. W., and Wand, M. D., 1990, *Phys. Rev. A*, **42,** 6087.
[16] Chan, T., Bahr, Ch., Heppke, G., and Garland, C. W., 1993, *Liq. Cryst.*, **13,** 667.
[17] Lushington, K. J., Kasting, G. B., and Garland, C. W., 1980, *J. Phys. Lett. (Paris)*, **41,** L-419.
[18] Yokoyama, H., 1988, *J. chem. Soc. Faraday Trans. II*, **84,** 1023.
[19] Iannacchione, G. S., Garland, C. W., Mang, J. T., and Rieker, T., to be published.
[20] Falicov, A., and Berker, A. N., 1996, *Phys. Rev. Lett.*, **76,** 4380, and references cited therein.
[21] Wen, X., Garland, C. W., and Heppke, G., 1991, *Phys. Rev. A*, **44,** 5064.